Advance Sustainable Science, Engineering and Technology (ASSET)
Vol. 8, No.1, January 2026, pp. 02601029-01 ~ 02601029-018
ISSN: 2715-4211 DOI: https://doi.org/10.26877/asset.v8i1.2672

Optimization of Off-Grid Solar Lighting Systems Using OEMOF Integrated with IoT Field Data — Case Study: Bukit Kunci, Indonesia

Eva Hertnacahyani Herraprastanti[1*], Berkah Fajar Tamtomo Kiono[1], Ismoyo Haryanto[1], Muchammad[1], Muhammad Safar Korai[2]

[1]Faculty of Technology, Universitas Diponegoro, Jl. Prof. Jacub Rais, Tembalang, Kec. Tembalang, Kota Semarang, Jawa Tengah 50275, Central Java, Indonesia

[2]Institute of Environmental Engineering and Management, Mehran UET Jamshoro, Sindh, Pakistan

*evahertnacahyaniherr@students.undip.ac.id

Abstract. The growing need for efficient night lighting in natural tourist destinations highlights the importance of reliable and sustainable energy solutions. This study analyzes the optimization of solar-based lighting at Bukit Kunci, Indonesia, using the Open Energy Modelling Framework (OEMOF) combined with real-time monitoring via the IoT ThingSpeak platform. Photovoltaic (PV) panel data recorded at 15-second intervals during February–July 2025, yielding 532,520 records, were cleaned and aggregated as input to model the interaction of PV, batteries, LED lights, inverters, and backup generators, to minimize lifecycle cost and energy loss. Results indicate that the current PV capacity (0.4 kWp) supplies less than 50% of lighting demand, with a high levelized cost of energy (≈9.2 USD/kWh) and low reliability (self-sufficiency 3–22%). Optimization through capacity expansion (≈224 modules, ≈1.25 kWh storage) eliminated load loss probability and reduced LCOE to ≈0.05 USD/kWh. This approach demonstrates OEMOF's potential to enhance system efficiency, ensure reliable night lighting, and support eco-tourism while offering replicability for rural destinations.

Keywords: OEMOF, off-grid systems, energy optimization, rural tourism energy, LCOE, IoT monitoring.

(Received 2025-09-03, Revised 2025-11-31, Accepted 2026-01-15, Available Online by 2026-01-31)

1. Introduction

The demand for reliable and sustainable night lighting in tourist destinations such as Bukit Kunci is increasing alongside tourism development, which requires both visitor comfort and safety. Conventional grid-based systems are often inefficient or unavailable in rural tourist areas, creating a need for lighting solutions that combine visual quality, reliability, and sustainability. Off-grid photovoltaic (PV) systems are a viable option, but their performance and cost-effectiveness depend strongly on proper system design and optimization.

Optimization frameworks such as the Open Energy Modelling Framework (OEMOF) provide a modular, transparent, and reproducible approach to designing integrated energy systems that include PV generation, storage, and loads, with explicit consideration of efficiency and cost [1–4]. OEMOF has been widely applied in large-scale or institutional energy planning, such as regional energy transitions [5], building retrofits [6,7], and decentralized system strategies [8,9]. However, the application of OEMOF to small-scale energy infrastructure related to the tourism sector is still relatively limited. Most previous research has focused more on urban or industrial contexts, so the application of OEMOF for micro-scale off-grid systems in rural tourism areas has not been widely explored. On the other hand, small-scale off-grid system analysis is generally more often done using other software, such as HOMER, which has become more established in integrated energy system analysis [10,11].

At the same time, the Internet of Things (IoT) enables real-time monitoring and control of energy systems. Platforms such as ThingSpeak can record and visualize high-frequency data (irradiance, voltage, current, temperature) that are valuable for model calibration and optimization. Numerous IoT systems have been developed for smart lighting and energy efficiency, including LoRaWAN-based lighting control [12] and low-cost monitoring architectures for campus-scale systems [13]. oT-based monitoring and control have become essential tools for achieving data transparency and operational efficiency in smart grids [14]. While ThingSpeak and similar platforms have proven effective for PV data analysis and simulation [15], their integration with techno-economic optimization models in the tourism energy context remains underexplored.

Recent studies in the hospitality sector have highlighted the benefits of smart monitoring for managing energy consumption and guest comfort [16] and optimizing hybrid renewable systems for tourist facilities [17]. Similarly, IoT-based street lighting control has been implemented in urban environments [18], and broader reviews emphasize IoT's potential for intelligent energy management in buildings and cities [19], [20]. Nevertheless, few works have systematically combined field IoT data with optimization models to design and evaluate energy systems for rural tourist sites.

This study bridges that gap by integrating OEMOF optimization with real-time IoT monitoring via ThingSpeak to evaluate and improve solar-powered lighting infrastructure. The research objectives are:

1. To demonstrate how high-frequency IoT data can improve the accuracy and realism of OEMOF-based optimization for small PV–battery systems;
2. To assess the techno-economic performance and life-cycle cost of solar lighting configurations, and
3. To evaluate the replicability of the proposed framework for similar off-grid rural tourism sites.

The novelty of this research lies in the integration of real-time IoT data streams with an open-source optimization framework to develop a reproducible, data-driven methodology for small-scale energy systems. The proposed approach provides a transparent pathway for enhancing energy efficiency, reliability, and sustainability of lighting infrastructure in rural tourism destinations such as Bukit Kunci, Indonesia.

2. **Methods**

2.1. Study Location

The study was conducted in Bukit Kunci, Blora Regency, Central Java, Indonesia (6°57.6′ S, 111°31.3′ E), a hilly natural tourist site known for panoramic views and night-time city lights. The area's elevation ranges from 100–500 m above sea level, with slopes of 5–20° influencing panel tilt and orientation. The climate is tropical with distinct rainy (November–March) and dry (April–October) seasons. According to BMKG data, the average daily solar irradiation is 5.2–5.5 kWh/m²/day, with average temperatures between 24–27 °C and humidity of 70–85 %, indicating good solar energy potential [21].

2.2. Data Acquisition and Processing

Real-time PV performance data were collected through an IoT-based monitoring system connected to the ThingSpeak platform. The setup included PZEM-017 energy meters and INA219 current sensors linked to a NodeMCU ESP8266 microcontroller.

Data were collected using a ThingSpeak-based IoT logger with 15-second sampling from February to July 2025. The monitoring system recorded irradiance, voltage, current, power, and cumulative energy from the PV subsystem.

Raw data contained 532,520 entries, of which 204,135 were invalid due to missing or negative readings in voltage, current, or power channels. Additionally, 21,608 zero-power anomalies were detected where irradiance exceeded 100 W/m² but PV power readings were near zero, indicating potential logger disconnections or sensor dropouts. After filtering and timestamp normalization (UTC+7), 328,385 valid records were retained, corresponding to 61.67 % completeness.

The existence of data anomalies in IoT-based PV monitoring systems is a common phenomenon, especially due to communication interference and dropout sensors in multivariate time series data. Guo et al. point out that this kind of anomaly needs to be addressed through a data filtering process so that the analysis of the energy system is not distorted by measurement artifacts. Thus, the data cleansing stage in this study is an important step before the data is used for performance analysis and system optimization [22,23].

Temporal anomaly analysis showed that most anomalies occurred in March (226 cases) and April 2025 (197 cases), coinciding with intermittent data-logger instability during the early deployment period. From May–July 2025, the number of anomalies dropped sharply (to < 90 per month) after on-site maintenance and cable tightening, confirming improved reliability of the data acquisition chain.

Cleaned data were aggregated into hourly averages for use as OEMOF model inputs. No gap-filling or interpolation was applied beyond anomaly removal to preserve data authenticity. Validation was cross-checked using BMKG solar radiation data for Blora and PLN tariff references for the economic model. The resulting hourly dataset ensured reliable input consistency for subsequent OEMOF simulations. The physical configuration of the monitoring system is shown in Figure 1.

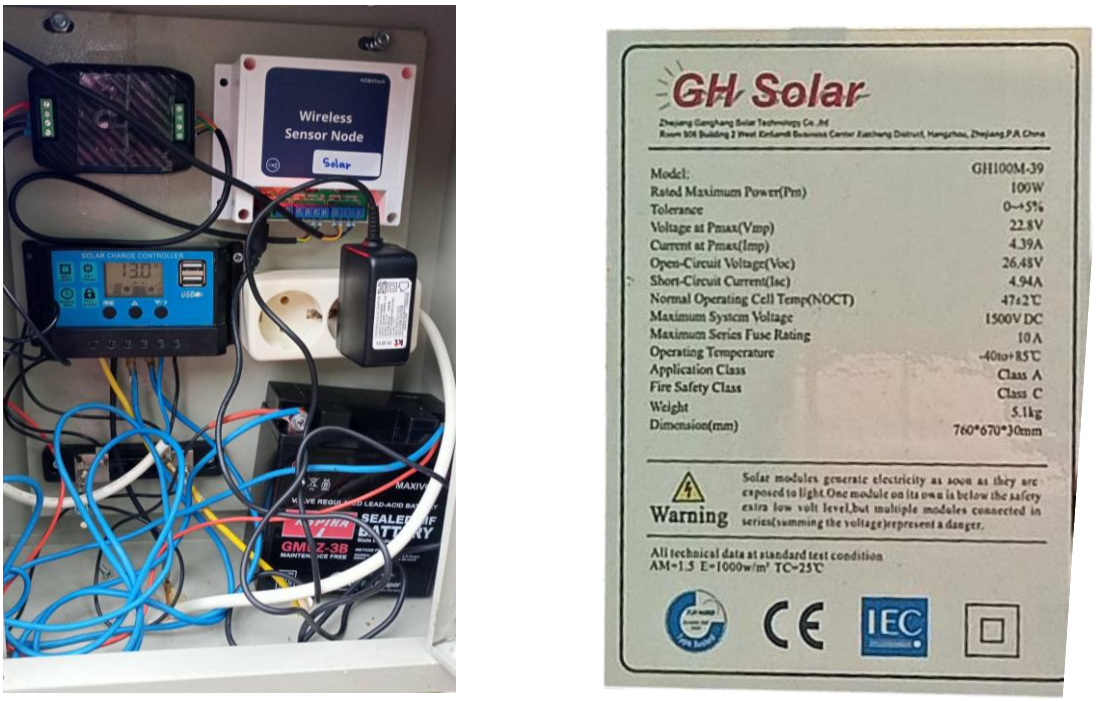

(a) (b)

Figure 1. (a) IoT-based PV control and data logging unit installed at Bukit Kunci; (b) GH Solar 100 Wp PV module label showing key specifications.

Figure 1 shows the configuration of the IoT-based monitoring unit installed at Bukit Kunci. The system includes a GH Solar 100 Wp panel, a PWM charge controller, and a VRLA 12 V 3 Ah battery housed within a waterproof box, connected to a wireless sensor node for continuous data transmission. The unit records irradiance, voltage, current, and power data every 15 seconds to the ThingSpeak cloud platform for real-time visualization and analysis.

2.3. OEMOF Model Development

The optimization of the solar lighting system in Bukit Kunci was conducted using the Open Energy Modeling Framework (OEMOF), an open-source Python library that models energy systems as directed graphs consisting of sources, sinks, storages, and transformers [3,24]. OEMOF enables transparent and modular optimization of techno-economic systems by representing each component and energy flow explicitly within a consistent mathematical structure.

In this study, the model structure reflects the actual off-grid PV–battery–inverter system installed on-site, integrating measured IoT-based power and irradiance data as time-series inputs. The model includes the following components:

1. Photovoltaic (PV) modules as energy sources.
2. Battery storage as energy buffers with round-trip efficiency and depth-of-discharge limits.
3. DC and AC buses interconnecting components.
4. Inverters and charge controllers as transformers.
5. LED-based lighting loads as energy sinks, modeled with hourly load profiles derived from IoT monitoring

2.3.1 Objective Function

The optimization problem in this study aims to minimize the total techno-economic cost of the off-grid solar lighting system using OEMOF. The system consists of photovoltaic (PV) modules, a lithium-ion battery pack, and an inverter supplying LED-based lighting. The optimization objective is to determine the optimal operation and sizing strategy that minimizes total operating and investment costs while ensuring a reliable power supply to the lighting load. The optimization problem is formulated as:

$$\min Z = \sum_{t=1}^{T} \sum_{i \in \{PV,bat,inv\}} C_i P_{i,t} + C_{om} \quad (1)$$

Where C_i represents the unit cost coefficient of component i(USD/kWh), and $P_{i,t}$ denotes the hourly power output or throughput of each component $i$at time step t. The component set {PV, bat, inv} refers to the photovoltaic array, battery storage, and inverter, respectively. C_{om} denotes the fixed operation and maintenance cost of the system. The objective function, therefore, seeks to minimize the total energy cost over the simulation horizon while maintaining energy balance between generation, storage, and load.

2.3.2 Constraints

The optimization is subject to several technical constraints that govern energy balance, storage dynamics, and operational limits of the photovoltaic (PV) and battery systems.

1. Energy Balance Constraint

The fundamental energy balance of the system ensures that, at each time step, the total generated energy equals the sum of consumption and storage changes, as expressed in Equation (2).

$$P_{PV,t} + P_{dis,t} = P_{LED,t} + P_{ch,t} \quad (2)$$

The notations are defined as follows:

$P_{PV,t}$ = Electrical power generated by the photovoltaic (PV) array at time t(W)

$P_{dis,t}$ = Power discharged from the battery storage at time t(W).

$P_{LED,t}$ = Power consumed by the lighting load (LED lamps) at time t(W).

$P_{ch,t}$ = Power used to charge the battery at time t(W).

This constraint ensures that, at every time step t, the total power generated by the PV array and the power discharged from the battery equals the total lighting demand and the power used for charging the battery.

2. Battery State of Charge (SoC) Dynamics

In the OEMOF-based model, the battery SoC represents the temporal energy balance within the storage component, governed by charge and discharge efficiencies as formulated in Equation (3).

$$SoC_t = SoC_{t-1} + \eta_{ch} P_{ch,t} - \frac{P_{dis,t}}{\eta_{dis}} \quad (3)$$

This equation represents the temporal evolution of the battery's state of charge (SoC), describing how stored energy in the battery changes at each time step t. The notations are defined as follows:

SoC_t = State of charge of the battery at time t(Wh or % of capacity).
SoC_{t-1} = State of charge of the battery at the previous time step.
η_{ch} = Charging efficiency of the battery (fraction, typically 0.9–0.95).
$P_{ch,t}$ = Charging power entering the battery at time t(W).
$P_{dis,t}$ = Power discharged from the battery at time t(W).
η_{dis} = Discharging efficiency of the battery (fraction, typically 0.9–0.95).

The first term SoC_{t-1} represents the stored energy at the previous timestep. The second term $\eta_{ch} P_{ch,t}$ adds the energy gained from PV charging, adjusted by the charging efficiency. The third term $\frac{P_{dis,t}}{\eta_{dis}}$ subtracts the energy discharged, accounting for losses during discharge.

This dynamic model ensures that the battery energy balance remains consistent throughout the simulation and allows OEMOF to optimize the charge/discharge schedule while respecting real-world efficiency losses.

3. Battery Capacity Limits

The allowable range of the battery's state of charge is constrained by its minimum and maximum capacity limits, ensuring safe and reliable operation of the storage system, as defined in Equation (4).

$$SoC_{min} \leq SoC_t \leq SoC_{max} \quad (4)$$

This inequality defines the allowable operating limits of the battery's state of charge (SoC) over time, ensuring safe and reliable battery operation throughout the simulation. The notations are defined as follows:

SoC_{min} = The minimum allowable state of charge, corresponding to the maximum depth of discharge (DoD). Operating below this level risks battery degradation or failure.
SoC_t = The minimum allowable state of charge, corresponding to the maximum depth of discharge (DoD). Operating below this level risks battery degradation or failure.
SoC_{max} = The maximum allowable state of charge, typically close to the nominal battery capacity (e.g., 100%), representing the upper energy storage limit.

This constraint ensures that the battery does not exceed its design capacity during charging and does not discharge beyond its safe operating threshold. Maintaining the SoC within these boundaries protects the battery's lifetime, prevents overcharging or deep discharging, and maintains realistic behavior in the OEMOF optimization model.

4. Depth of Discharge (DoD) Relation

The minimum allowable state of charge of the battery is determined by its depth of discharge (DoD), which defines the fraction of total capacity that can be safely utilized without accelerating degradation, as shown in Equation (5).

$$SoC_{min} = (1 - DoP) \times E_{bat} \quad (5)$$

Where E_{bat} denotes the nominal battery energy capacity (Wh). The depth of discharge (DoD) is a design parameter defining the maximum usable fraction of stored energy.

5. PV Generator limits

The maximum power output of the photovoltaic (PV) array is constrained by its conversion efficiency, active surface area, and the incident solar irradiance at a given time, as expressed in Equation (6).

$$P_{PV,t} \leq \eta pv \,.\, A_{PV} \,.\, G_t \quad (6)$$

Where $P_{PV,t}$ is the PV output power at time t(W), ηpv is the PV conversion efficiency, A_{PV} is the total active panel area (m²), and G_t is the solar irradiance (W/m²) at time t. This ensures that the generated PV power never exceeds the physical capacity determined by panel area and local solar resource.

2.3.3 Mathematical Modelling of Components

This section describes the mathematical and technical formulations of each component in the off-grid solar lighting system model. The model includes three main subsystems: photovoltaic (PV) generation, battery storage, and the inverter that supplies the AC lighting load. Each subsystem is represented in OEMOF as a node with specific techno-economic parameters and efficiency constraints.

1. Photovoltaic (PV) Subsystem

The PV subsystem converts solar irradiance into electrical power according to:

$$P_{PV,t} = \eta pv \,.\, A_{PV} \,.\, G_t \quad (7)$$

The physical configuration of the PV subsystem is presented in Fig. 2(b), illustrating the wiring, charge controller, and dual-module (2 × 100 Wp) array setup used in the field installation.

Table 1. Technical and Economic Specifications of the Solar Panel

Parameter	Symbol (Unit)	Value	Description / Source
Rated capacity	$P_{PV,cap}$ (WP)	200	2 modules × 100 Wp (field prototype)
Module efficiency	ηPV (%)	16.5	Manufacturer (GH Solar GH100M-39)
Effective system efficiency	$\eta PV, eff$ (%)	15.7	Includes derating (0.95)
Module area	A_{PV} (m²)	0.51	From label dimensions
Mounting tilt/orientation	–	15° / North-facing	Field installation
System derating factor	–	0.95	Wiring & dust losses
Investment cost	$C_{PV,cap}$ (USD/kWp)	480	Field procurement
O&M cost	$C_{PV,om}$ (%CAPEX/yr)	1	Assumed annual maintenance

2. Battery Storage Subsystem

Battery storage is modelled dynamically based on its charging and discharging behavior, as formulated in Equations (4–5). The battery's state of charge (SoC) evolves with time according to:

$$SoC_t = SoC_{t-1} + \eta_{ch} P_{ch,t} - \frac{P_{dis,t}}{\eta_{dis}} \quad (8)$$

With operational bounds defined by equation (4), and the relationship between minimum SoC and Depth of Discharge (DoD) defined by equation (5). Fig. 3 presents the configuration of the Li-ion battery pack used in the system, with detailed specifications summarized in Table 3.

Figure 2. Li-ion battery pack used in the system

The battery subsystem was modeled with charge/discharge efficiency (ηch, ηdis) and state-of-charge (SoC) limits following the OEMOF storage formulation. The expected lifetime of the $LiFePO_4$ battery (5–7 years) accounts for typical cycle degradation and capacity fade characteristics of lithium-ion cells, consistent with empirical aging models reported by Madani et al. [25].

Table 2. Technical and Economic Specifications of the Battery Subsystem

Parameter	Symbol (Unit)	Value	Description / Source
Nominal energy capacity	E_{bat} (Wh)	158.8	(E = V \times C)
Battery type/chemistry	–	Li-ion (18650 cells)	Field-installed specification
Charging efficiency	η_{ch}	0.95	Typical for Li-ion systems
Discharging efficiency	η_{dis}	0.90	Typical for Li-ion systems
Depth of discharge	DoD	0.8 (80 %)	Operational limit to extend cycle life
Investment cost	$C_{bat,\ cap}$ (USD/kWh)	93	Field procurement (≈ IDR 1,400,000)
O&M cost	$C_{bat,om}$ (%CAPEX/yr)	2 %	Periodic controller and terminal check
Lifetime assumption	–	5 years	For the annualized cost in the OEMOF model

3. Inverter Subsystem

The inverter converts DC energy from PV and battery sources to AC power for the LED load. Its efficiency is modelled as equation (9).

$$P_{inv,t} = \eta_{inv} \times (P_{PV,t} + P_{dis,t}) \quad (9)$$

Where:

$P_{inv,t}$ = is the AC output power at time t,

η_{inv} = is the inverter conversion efficiency.

Figure 4 presents the configuration of the inverter used in the system.

Figure 4. The Inverter Used in The System

The configuration and labeling of the DC–AC inverter used in the solar lighting prototype are shown in Fig. 3(b). The inverter converts the 12 V DC output from the battery to 220 V AC for LED lighting loads. The corresponding technical and economic specifications are summarized in Table 3.

Table 3. Technical and Economic Specifications of the Inverter Subsystem

Parameter	Symbol (Unit)	Value	Description / Source
Rated output power	$P_{inv,r}$ (W)	1000	Continuous AC output
DC input / AC output voltage	V_{DC} / V_{AC} (V)	12 / 220	Compatible with battery bank
Output frequency	f (Hz)	50	Standard for the Indonesian grid
Conversion efficiency	η_{inv}	0.90	Manufacturer's typical range
Investment cost	$C_{inv,\,cap}$ (USD/kW)	172	Field procurement (≈ IDR 2,600,000)
O&M cost	$C_{inv,\,om}$ (%CAPEX/yr)	1 %	Periodic cleaning & inspection
Expected lifetime	–	5 years	For annualized OEMOF modeling

2.3.4 OEMOF Simulation Framework and Assumptions

The optimization was implemented in Python 3.10 using the Open Energy Modelling Framework (OEMOF) library. OEMOF represents the energy system as a directed graph, where each node corresponds to a component (e.g., PV, battery, inverter, or lighting load) and edges represent the energy flow between them. The optimization aims to minimize total techno-economic cost, formulated in Section 2.3.1, while maintaining the physical and operational constraints defined in Section 2.3.2.

2.3.4.1 Simulation Horizon and Temporal Resolution

Measured PV and electrical data were collected at 15-second intervals from January to July 2025 using the installed IoT-based data logger. After cleaning and validation, these data were aggregated into hourly averages ($\Delta t = 1$ h) to ensure computational efficiency and compatibility with OEMOF's standard time-series structure. The simulation horizon covered the full 7-month observation period (January–July 2025), which was treated as a representative operating year for the local climate of Bukit Kunci. This period includes both wet and dry seasons, allowing the model to capture realistic variations in solar irradiance and system performance under actual field conditions.

2.3.4.2 Model Structure and Assumptions

The OEMOF model consists of three primary subsystems—PV, battery, and inverter—interconnected through DC and AC buses. The main assumptions are as follows:

1. Energy balance is enforced at every time step, ensuring supply equals demand.
2. PV generation depends on measured irradiance and temperature; no synthetic weather data are used.
3. Battery degradation effects are neglected within the 7-month simulation horizon, assuming constant efficiency.
4. Economic parameters (CAPEX and OPEX) are derived from field procurement costs and annualized using a 5% discount rate. The capital and operational expenditures were calculated based on the installed

capacity of each subsystem using the following relations:

$$CAPEX = \sum_{I}(C_{i,cap} \times P_i) \; ; \; PPEX = \sum_{I}(C_{i,om} \times P_i) \tag{10}$$

Where $C_{i,\,cap,}$ and $C_{i,\,om}$ denote the specific capital and annual operation & maintenance costs (USD per unit capacity) of component *i* (PV, battery, inverter), and P_i is its installed capacity. These values were derived from field procurement data and standardized techno-economic references [22]. The resulting total cost is annualized at a 5 % discount rate and used in the subsequent LCOE formulation (Equation 6).

5. Operational lifetime assumptions: PV = 15 years, Battery = 5 years, Inverter = 5 years.
6. No load shedding is allowed; unmet demand incurs a high penalty cost (λ).

The model was executed using OEMOF's solph optimization package with the CBC solver, performing linear programming (LP) optimization to obtain the least-cost configuration and operational schedule. The structure of the OEMOF model representing the off-grid lighting system is illustrated in Figure 4, showing the interactions among PV generation, battery storage, and inverter subsystems.

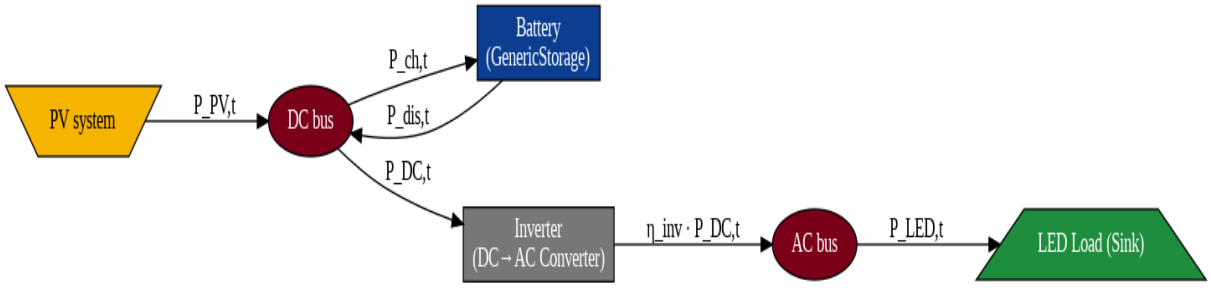

Figure 4. PV generation, battery storage, and inverter subsystems modelling by OEMOF

Figure 4 illustrates the OEMOF-based energy flow diagram of the proposed off-grid PV lighting system. The PV array acts as a DC energy source that supplies power to a DC bus. The generated energy can either charge the battery storage or be converted to AC via the inverter to supply the LED lighting load. The battery operates as an energy buffer, storing excess PV energy during the daytime and discharging when solar generation is insufficient. The inverter converts DC power into AC power with an efficiency $\eta_{inv,}$ ensuring a continuous supply to the AC load.

3. Results and Discussion

3.1. Data Visualization from ThingSpeak

The monitoring data of the PV system in Bukit Kunci collected through the IoT platform ThingSpeak is analyzed to obtain an overview of the potential of solar energy and the actual performance of the system. Two forms of visualization are shown to highlight the temporal variation and physical relationship between solar radiation and panel output power.

The results of ThingSpeak-based data visualization in this study are consistent with previous studies that show that the platform is able to reliably provide PV parameter data for small-scale systems. Sutikno et al.[26] report that the integration of NodeMCU ESP8266 and ThingSpeak supports real-time and historical PV monitoring at a low cost. Different from the study, this study uses IoT data as the main input in OEMOF-based energy system optimization, so that monitoring data plays a direct role in system evaluation and design.

3.1.2 Temporal Variations of Energy and Insolation.

Figure 1 shows that at Bukit Kunci (Jan–Jul 2025), solar insolation ranges from 2,000–6,000 Wh/m² on sunny days but drops sharply in cloudy/rainy conditions. PV output is very low, averaging 20–60 Wh/day with occasional peaks above 100 Wh. From May to early June, output was nearly zero despite

recorded insolation, suggesting operational issues or data logger problems. Overall, PV capacity is far below the site's solar potential.

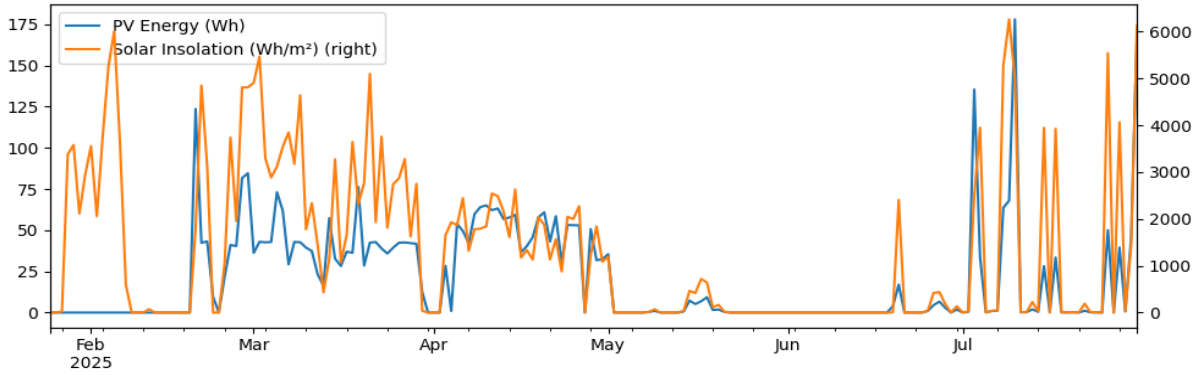

Figure 5. Temporal Variations of Energy and Insolation

3.1.3 The Relationship of Irradiance and PV Power

Data is aggregated into monthly averages to analyze seasonal trends and serve as input for the OEMOF optimization model. Climate data from BMKG and NASA POWER validate field measurements, while PLN tariff data support economic analysis. Data cleaning, processing, and aggregation are performed in Python (Google Colab) using pandas for manipulation and matplotlib for visualization.

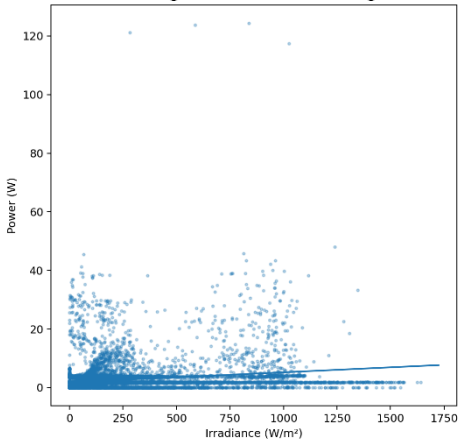

Figure 6. Scatter plot between irradiance (W/m²) and PV output power

These two visualizations (figures 1 and 2) provide an important basis for the optimization process using OEMOF. The temporal pattern of insolation is used to construct the input profile of the solar energy source, while the scatter plot highlights the low actual efficiency of the system. The combination of the two justifies the need for an optimization strategy based on energy storage to ensure the availability of electricity during curfews in the Bukit Kunci tourist area.

3.1.4 Night load profile.

Figure 3 shows the night lighting load profile.

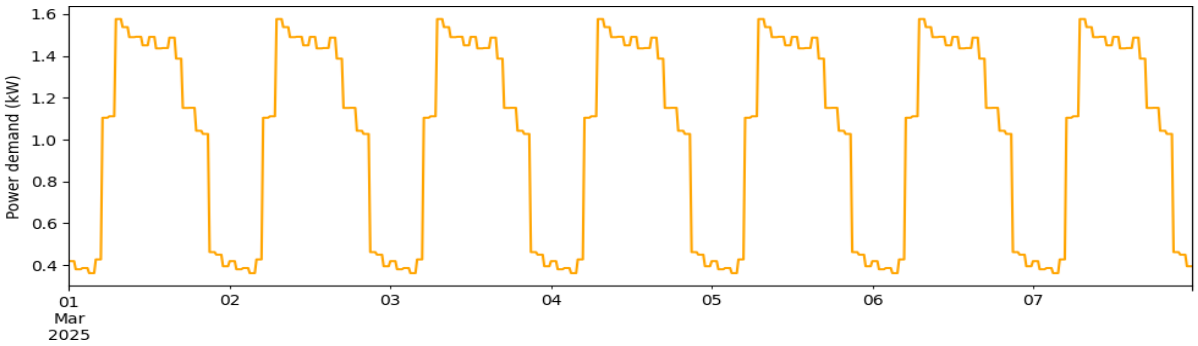

Figure 7. The night lighting load profile

The lighting load is constant at about 0.06 kW from 18:00–06:00 and zero during the day. Data from February–July 2025 shows a consistent daily on/off cycle, confirming that the tourist lighting demand is stable and requires a continuous nightly energy supply.

3.1.5 Supply and Demand Gap

Figure 8 presents a comparison of PV supply and energy demand at 15-minute resolution.

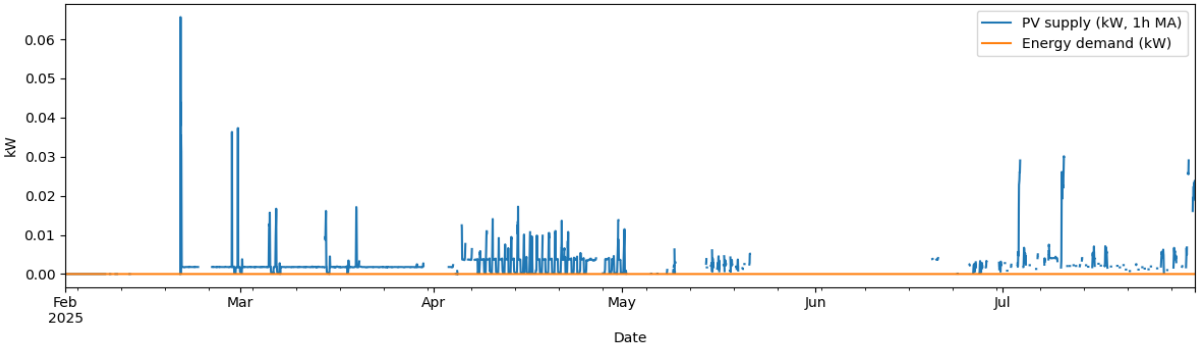

Figure 8. *Supply and Demand Gap*

PV output is only available during the day with fluctuating values, while the lighting load remains constant at night. This creates a temporal mismatch: surplus energy in the daytime and a deficit at night. This highlights the need for an energy storage system (battery) to balance supply and demand.

3.2 The results of the optimization simulation

3.2.1 Energy output efficiency

The simulation compares the PV system (4 modules @100 Wp) with the demand of 15 LED lamps (≈0.9 kWh/day). The lamp load is stable, while PV output averages only 0.2–0.3 kWh/day, supplying less than 50% of lighting needs on most days, as shown in Figure 9.

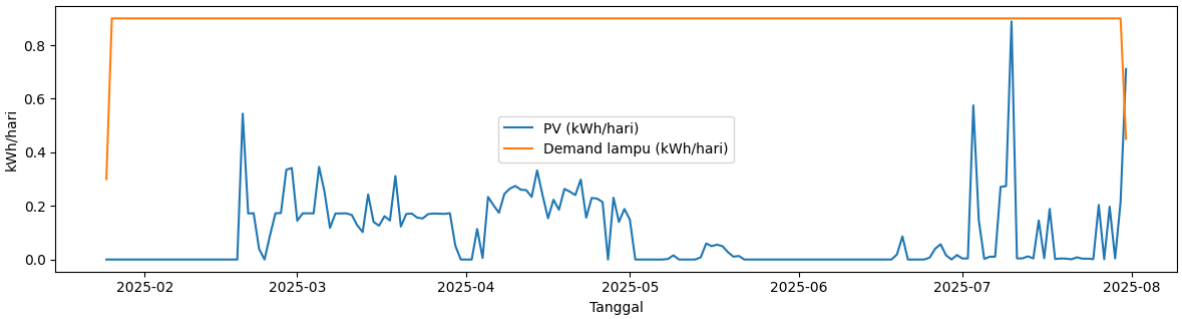

Figure 9. Daily Energy: PV Vs Demand Lamps

During sunny periods (late March and July), PV can generate 0.5–0.8 kWh/day, covering 60–80% of lighting demand. However, in low irradiation months (May–June), PV supply drops sharply to <0.1 kWh/day, requiring almost all loads to be supported by backups (grid or batteries). This shows that solar energy is effective but highly dependent on seasonal conditions.

3.2.2 Energy Costs

The LCOE calculation is carried out with a 20-year horizon and a discount rate of 8%. The investment value of the PV system is 4×100 Wp (0.4 kWp) included as an initial cost, with an O&M of 1% per annum. The results of the calculation are shown in Table 4.

Table 4. LCOE calculation results of a 4×100 Wp PV system for lamp load

Parameter	Value
NPV total cost (20 years)	$746,76
Rated PV energy (kWh)	321
LCOE_gen (USD/kWh)	2,33
Spent PV energy (kWh)	81
LCOE_used (USD/kWh)	9,24

These results show that the cost of solar energy generated (LCOE_gen) is ≈ $2.33/kWh, while the cost of energy actually utilized for lighting (LCOE_used) reaches ≈ $9.24/kWh. This value is much higher than the price of conventional electricity because the energy recorded is relatively small due to the limitations of the data logger (only a portion of the day is recorded).

3.2.3. System Reliability

The reliability of the system is evaluated through a state-of-charge (SoC) analysis of the battery during the period February–July 2025. The SoC graph in the following image shows the charging and discharging patterns of the battery due to the imbalance between the PV energy availability and the load to be met.

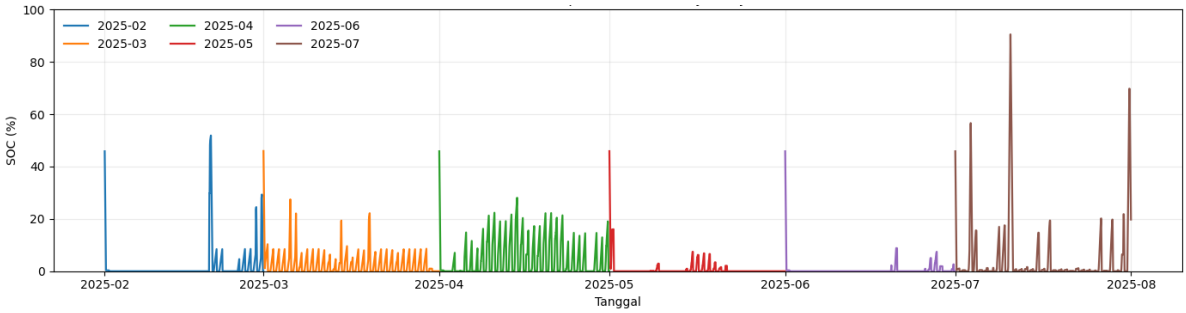

Figure 10. SoC Battery (% capacity-overlay Feb-July 2025)

The PV-battery system rarely reaches full SoC, often stays low, and frequently undergoes deep discharge, risking battery life and supply reliability. Although SoC rises slightly in high-radiation months, the system still struggles to ensure a continuous supply. With LOLP at ≈96% and self-sufficiency under 5%, its reliability is very limited, requiring optimization through added PV capacity, more batteries, or backup integration.

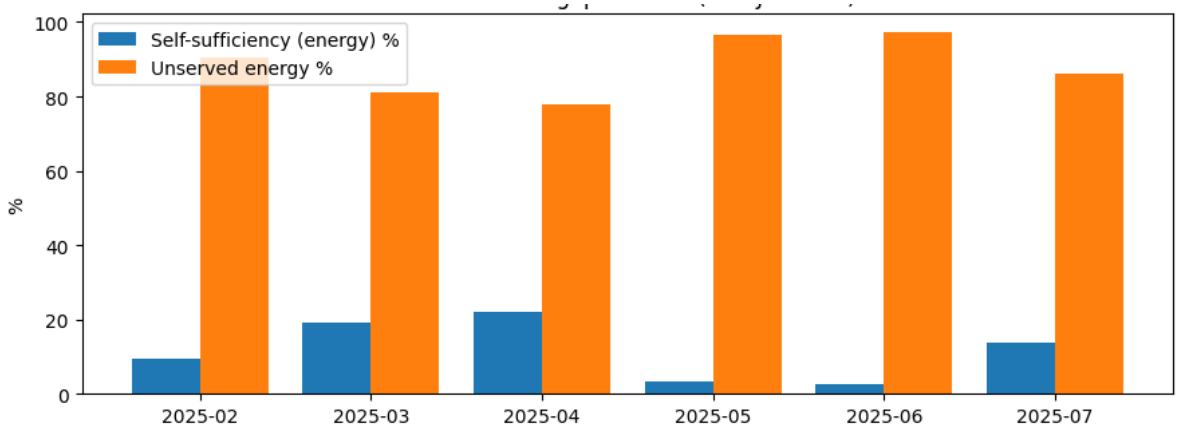

Figure 11. Energy Indicators per Month (Feb-July 2025)

The reliability of the PV-battery system in Bukit Kunci is still low, shown to be self-sufficient at only 3–22% throughout February-July 2025. The majority of load energy is unserved (78–97%), so the dependence on backup sources remains high. This condition confirms the need to increase PV and battery capacity so that the system can more reliably serve night loads.

3.3 Implications for Tourism Infrastructure

The reliability of the electrical energy supply for nighttime lighting in Bukit Kunci is very important for the comfort of visitors and the image of tourist destinations. The results of this simulation show that the combination of PV and batteries can provide reliable and sustainable electricity. With high self-sufficiency, this system has the potential to reduce long-term operational costs while supporting eco-tourism branding.

3.4 Comparison before & after optimization

The conditions before optimization (Baseline) can be seen in Figure 12.

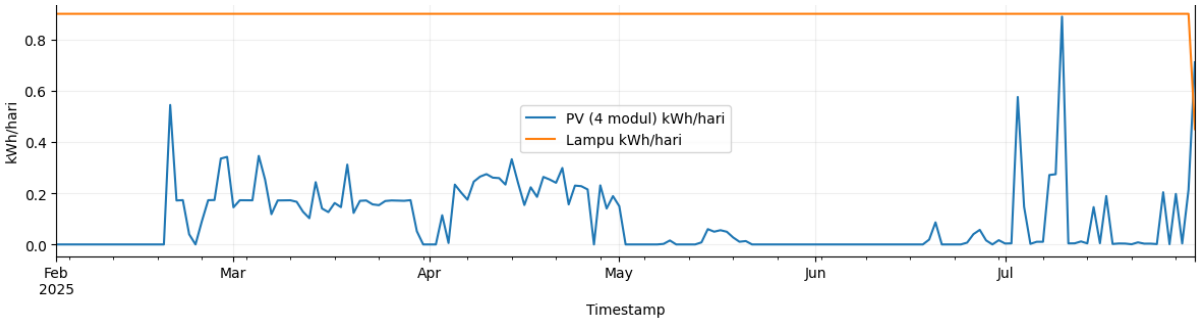

Figure 12. Before optimization (Baseline)

The baseline PV system with 4 modules produces only 0.0–0.4 kWh/day, far below the lamp demand of ≈0.85 kWh/day and often nearly zero. This results in large energy deficits, leaving most lighting needs unmet from February to July 2025. Occasional spikes in late February and July occur, but are still insufficient, making the system unable to sustain lighting needs and dependent on external sources.

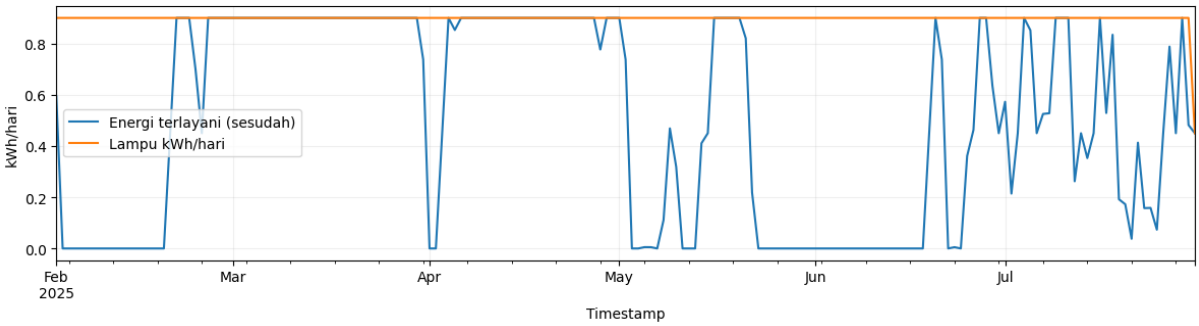

Figure 13. After OEMOF Optimization

After optimization (PV ≈224 modules, battery ≈1.25 kWh), energy production increased sharply, meeting most daily lighting needs. The battery improved supply continuity, though extreme conditions caused occasional drops. In contrast, the baseline with 4 PV modules produced only ≈34.3 kWh/year, with ≈8.6 kWh/year used for lamps, leading to low self-sufficiency and a high LCOE (≈9.2 USD/kWh). OEMOF optimization enabled better PV utilization and battery charging, reducing losses, achieving 100% self-sufficiency in April with LOLP = 0%, and lowering LCOE to ≈0.05 USD/kWh, making the system reliable and economical.

Table 5. Summary of Key Findings

Indicator	Value
PV energy (4 modules, annualized)	≈ 34,3 kWh / year
Lamp load (annualization)	≈ 54,7 kWh / year
LOLP (*Loss of Load Probability*)	0% (lamp load is always served)
LCOE (*Levelized Cost of Energy*)	Used energy

3.5 Sensitivity and Uncertainty Analysis

In the context of an economic analysis of the energy system, Capital Expenditure (CAPEX) [27] refers to the initial investment cost for the purchase and installation of system components, while Operational Expenditure (OPEX) includes annual operating and maintenance costs [27]. Meanwhile, the Levelized Cost of Energy (LCOE) [28] describes the average cost of electrical energy production per unit kWh over the life of a project, which is calculated based on the total investment and operating costs compared to the total energy produced, as expressed in Equation (10).

$$LCOE = \frac{\sum_{t=1}^{n} \frac{C_t}{(1+r)^t}}{\sum_{t=1}^{n} \frac{E_t}{(1+r)^t}} \quad (11)$$

Where C_t denotes the annualized investment, replacement, and operational costs at year t, E_t is the corresponding annual energy output, r is the discount rate, and n is the system lifetime. The LCOE value is used as a key indicator in assessing the economic feasibility and sensitivity of the system to changes in technical and financial parameters [29].

Sensitivity analysis was conducted to evaluate the uncertainty of the key parameters in the optimization results of the off-grid solar PV technology developed in this study. Varied parameters include investment cost (CAPEX ± 20%), discount rate (4% – 10%), battery life (3 – 7 years) [25], and solar irradiation variation (± 10%).

The results of the analysis showed that LCOE values were most sensitive to CAPEX changes and discount rates, with values ranging from 59 to 86 USD/kWh from a baseline of 64.22 USD/kWh.

A 20% decrease in CAPEX lowers LCOE by about 8%, while a 20% increase in CAPEX increases LCOE by 35%. An increase in the discount rate also increases the LCOE because it lowers the present

value of the energy produced, while a longer battery life lowers the LCOE due to reduced component replacement costs. In this context, the effect of component degradation is implicitly reflected in the battery lifetime scenarios, which represent gradual performance decline over time.

The summarized effects of each parameter variation on the Levelized Cost of Energy (LCOE) are presented in Table 6, which highlights the relative influence of CAPEX, discount rate, battery lifetime, and solar irradiance on the system's overall economic performance.

Table 6. Sensitivity of Key Parameters on LCOE

Parameter	Variation	LCOE (USD/kWh)	Δ from baseline (%)	Interpretation
PV CAPEX	–20 % (80 %)	59.35	–7.6	Lower investment slightly decreases LCOE
	+20 % (120 %)	86.51	+34.7	Higher CAPEX proportionally increases LCOE.
Discount rate (r)	4 % → 10 %		+10 – 20	Higher discount rates raise LCOE due to lower Net Present Value (NPV) of energy.
Battery lifetime	3 → 7 years		–20 – 30	Longer lifetime reduces LCOE by minimizing replacement cost
Solar irradiance	+10 %	59 – 69	± 5 – 8	Irradiance variability moderately affects LCOE.

Variations in solar irradiation have only a moderate effect (< 10%), suggesting that meteorological uncertainty is not very dominant on the economic outcomes of the system. Overall, these results confirm that investment cost factors and financial parameters are the main determinants of the economic viability of off-grid solar PV systems. So, taking into account the results of this sensitivity, efforts to reduce the cost of key components (especially PV modules and inverters) and optimize battery life will have the most significant impact on lowering the LCOE of the system in the future. The corresponding trend of CAPEX impact on LCOE is depicted in Figure 14.

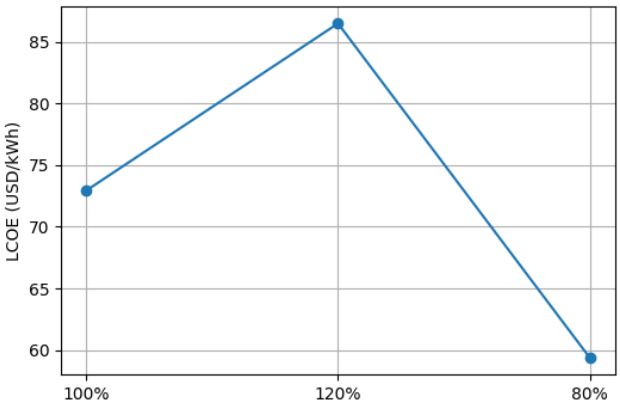

Figure 14. LCOE Sensitivity to CAPEX (±20%)

The figure illustrates the nearly linear relationship between investment cost (CAPEX) and LCOE. A 20 % increase in CAPEX raises the LCOE by approximately 35 %, while a 20 % decrease reduces it by about 8 %. This confirms that investment cost exerts the most significant influence on the levelized cost of electricity compared with other parameters. The LCOE value obtained in this study needs to be understood as an estimate that depends on the financial and technical assumptions used. The literature shows that LCOE is highly sensitive to parameters such as discount rates, system lifespan, and effective capacity, so small variations on those assumptions can result in significant cost differences. Therefore, the interpretation of the LCOE results needs to be accompanied by an analysis of uncertainty and sensitivity to avoid misleading conclusions [30].

4. Conclusion

This study shows the application of the Open Energy Modelling Framework (OEMOF) integrated with IoT-based PV data to optimize off-grid solar lighting systems in Bukit Kunci, Indonesia. The results show that the combination of OEMOF optimization and actual field data allows for a more accurate evaluation of system size, performance, and cost efficiency under real-world environmental conditions.

The configuration of the optimization results results in a balance between reliability and cost, with a lower Levelized Cost of Energy (LCOE) than the initial condition. Sensitivity analysis showed that the most influential factors on the economics of the system were the cost of investment (CAPEX) and discount rates, while variations in solar radiation and component degradation had a relatively smaller influence.

However, there are some limitations that need to be noted. The data used only covers a seven-month period (January–July 2025), and the possibility of data logger anomalies can lead to minor uncertainty in the results. These findings provide a strong indication of the effectiveness of the methods used, but further validation is still needed to ensure the results are comprehensive.

The next steps of the research will focus on the collection of long-term data to fully capture seasonal variations, advanced sensitivity analysis of the degradation of components and financial parameters, and field implementation of the optimization design results to verify their performance in real terms.

In addition, future research can integrate artificial intelligence (AI/ML) to predict load patterns based on tourism activities, as well as apply smart tourism concepts such as real-time monitoring, automated demand response, and digital tourism information systems. This approach is expected to strengthen the sustainability of renewable energy while enhancing a smart and sustainable ecotourism experience.

Acknowledgements

Acknowledgements, appreciation, and thanks are given to the Diponegoro University campus, all my promoters, and also to my colleagues from the Sekolah Tinggi Teknologi Ronggolawe.

References

[1] Hilpert S, Kaldemeyer C, Krien U, et al. The Open Energy Modelling Framework (oemof) - A novel approach in energy system modelling. Energy Strateg Rev 2018;22:16–25. https://doi.org/10.1016/j.esr.2018.07.001.

[2] Candas S, Muschner C, Buchholz S, et al. Code exposed: Review of five open-source frameworks for modeling renewable energy systems. Renew Sustain Energy Rev 2022;161:112272. https://doi.org/10.1016/j.rser.2022.112272.

[3] Hilpert S, Günther S, Söthe M. oemof.tabular – Introducing Data Packages for Reproducible Workflows in Energy System Modeling. J Open Res Softw 2021;9:1–9. https://doi.org/10.5334/JORS.320.

[4] Hilpert S, Kaldemeyer C, Krien U, et al. The Open Energy Modelling Framework (oemof) - A new approach to facilitate open science in energy system modelling. Energy Strateg Rev 2018;22:16–25. https://doi.org/10.1016/j.esr.2018.07.001.

[5] Maruf MNI. A novel method for analyzing highly renewable and sector-coupled subnational energy systems-case study of schleswig-holstein. Sustain 2021;13. https://doi.org/10.3390/su13073852.

[6] Hillen M, Schönfeldt P, Groesdonk P, et al. Integration of a Europe-wide public building database with retrofit strategies and a thermal inertia model into an open-source optimization framework. IOP Conf Ser Earth Environ Sci 2024;1363. https://doi.org/10.1088/1755-1315/1363/1/012013.

[7] Fleischmann J, Delgado Arroyo L, Dunks C, et al. Site-tailored configuration of integrated water-energy-food-environment systems using open software - case study of two Colombian sites. Energy Nexus 2025;19:100507. https://doi.org/https://doi.org/10.1016/j.nexus.2025.100507.

[8] Limpens G, Moret S, Jeanmart H, et al. EnergyScope TD: A novel open-source model for

regional energy systems. Appl Energy 2019;255:113729. https://doi.org/10.1016/j.apenergy.2019.113729.
[9] Muthukumaran G, Passos MV, Gong J, et al. Decentralized solutions for island states: Enhancing energy resilience through renewable technologies. Energy Strateg Rev 2024;54:101439. https://doi.org/10.1016/j.esr.2024.101439
[10] Niringiyimana E, Wanquan S, Dushimimana G, et al. Hybrid Renewable Energy System Design and Optimization for Developing Countries Using HOMER Pro: Case of Rwanda. 2023 7th Int. Conf. Green Energy Appl. ICGEA 2023, Zhejiang: IEEE Xplore; 2023, p. 72–6. https://doi.org/10.1109/ICGEA57077.2023.10125739.
[11] Bahramara S, Moghaddam MP, Haghifam MR. Optimal planning of hybrid renewable energy systems using HOMER: A review. Renew Sustain Energy Rev 2016;62:609–20. https://doi.org/10.1016/j.rser.2016.05.039.
[12] Cheikh I, Aouami R, Sabir E, et al. Multi-Layered Energy Efficiency in LoRa-WAN Networks: A Tutorial. IEEE Access 2022;10:9198–231. https://doi.org/10.1109/ACCESS.2021.3140107.
[13] Rhesri A, Bennani R, Maissa Y Ben, et al. Development of a low-cost Internet of Things architecture for energy and environment monitoring in a University Campus. Proc - 2023 Int Conf Futur Internet Things Cloud, FiCloud 2023 2023:181–5. https://doi.org/10.1109/FiCloud58648.2023.00034.
[14] Xiong L. Harnessing personal data from Internet of Things: Privacy enhancing dynamic information monitoring. 2015 Int. Conf. Collab. Technol. Syst., IEEE; 2015, p. 37–37. https://doi.org/10.1109/CTS.2015.7210393.
[15] Fotiou N, Halkiopoulos C, Antonopoulou H. Enhancing Tourism Sustainability Through Blockchain, AI, and Smart Technologies. A Comprehensive Analysis, 2025, p. 193–227. https://doi.org/10.1007/978-3-031-78471-2_8.
[16] Valett L, Bollenbach J, Keller R. Empowering sustainable hotels: a guest-centric optimization for vehicle-to-building integration. Energy Informatics 2024;7. https://doi.org/10.1186/s42162-024-00400-9.
[17] Hajinejad A, Seraj F, Jahangir MH, et al. Economic optimization of hybrid renewable energy systems supplying electrical and thermal loads of a tourist building in different climates. Front Built Environ 2023;8:1–17. https://doi.org/10.3389/fbuil.2022.969293.
[18] Mustafa ATM, Chowdhury M, Sultana J, et al. XXX-X-XXXX-XXXX-X/XX/$XX.00 ©20XX IEEE IoT-based Efficient Streetlight Controlling, Monitoring and Real-time Error Detection System in Major Bangladeshi Cities n.d.
[19] Nikpour M, Behvand P, Jafarzadeh H, et al. Intelligent Energy Management in Smart Cities : Leveraging IoT and Machine Learning for Optimizing Complex Networks and Systems 1-Introduction. ArXiv Prepr ArXiv230605567 2023:1–49.
[20] Witczak D, Szymoniak S. Review of Monitoring and Control Systems Based on Internet of Things. Appl Sci 2024;14. https://doi.org/10.3390/app14198943.
[21] Bangowan P. Desa Wisata Bangowan Kecamatan Jiken Kabupaten Blora Provinsi Jawa Tengah. 2020.
[22] Guo H, Zhou Z, Zhao D, et al. EGNN : Energy-E cient Anomaly Detection for IoT Multivariate Time Series Data Using Graph Neural Network 2023:1–15.
[23] Guo H, Zhou Z, Zhao D. GNN-Based Energy-Efficient Anomaly Detection for IoT Multivariate Time-Series Data. ICC 2023 - IEEE Int Conf Commun 2023:2492–7. https://doi.org/10.1109/ICC45041.2023.10278988.
[24] Ni S, Brockmann G, Darbandi A, et al. Modelling and optimization of a decarbonized heat supply in suburban areas using the Open Energy Modelling Framework. 37th Int Conf Effic Cost, Optim Simul Environ Impact Energy Syst ECOS 2024 2024;3:2230–9. https://doi.org/10.52202/077185-0191.
[25] Madani SS, Shabeer Y, Allard F, et al. A Comprehensive Review on Lithium-Ion Battery Lifetime Prediction and Aging Mechanism Analysis. Batteries 2025;11:1–68.

https://doi.org/10.3390/batteries11040127
[26] Sutikno T, Purnama HS, Pamungkas A, et al. Internet of things-based photovoltaics parameter monitoring system using NodeMCU ESP8266 2021;11:5578–87. https://doi.org/10.11591/ijece.v11i6.pp5578-5587
[27] Bovera F, Schiavo L Lo, Vailati R. Combining Forward-Looking Expenditure Targets and Fixed OPEX-CAPEX Shares for a Future-Proof Infrastructure Regulation: the ROSS Approach in Italy. Curr Sustain Energy Reports 2024;11:105–15. https://doi.org/10.1007/s40518-024-00239-4
[28] Almas, Sundaram S. Impact of Field Degradation Rates on the Levelized Cost of Energy (LCOE) for a roof-top Solar PV System. 2025 IEEE 53rd Photovolt. Spec. Conf., IEEE; 2025, p. 0564–7. https://doi.org/10.1109/PVSC59419.2025.11133123.
[29] Emblemsvåg J. Rethinking the "Levelized Cost of Energy": A critical review and evaluation of the concept. Energy Res Soc Sci 2025;119:103897. https://doi.org/10.1016/j.erss.2024.103897.
[30] Emblemsvåg J. Energy Research & Social Science Rethinking the " Levelized Cost of Energy " : A critical review and evaluation of the concept. Energy Res Soc Sci 2025;119:103897. https://doi.org/10.1016/j.erss.2024.103897.